

## RESEARCH ARTICLE

# Mycobacterial PPE13 activates inflammasome by interacting with the NATCH and LRR domains of NLRP3

Yang Yang<sup>1</sup> | Pianpian Xu<sup>1</sup> | Ping He<sup>2</sup> | Fushan Shi<sup>3</sup> | Yiran Tang<sup>1</sup> | Chiyu Guan<sup>1</sup> | Huan Zeng<sup>1</sup> | Yingshan Zhou<sup>1</sup> | Quanjiang Song<sup>1</sup> | Bin Zhou<sup>1</sup> | Sheng Jiang<sup>1</sup> | Chunyan Shao<sup>1</sup> | Jing Sun<sup>1</sup> | Yongchun Yang<sup>1</sup> | Xiaodu Wang<sup>1</sup> | Houhui Song<sup>1</sup>

<sup>1</sup>College of Animal Science and Technology, College of Veterinary Medicine, Key Laboratory of Applied Technology on Green-Eco-Healthy Animal Husbandry of Zhejiang Province, Zhejiang Provincial Engineering Laboratory for Animal Health Inspection and Internet Technology, Zhejiang A&F University, Hangzhou, China

<sup>2</sup>National Center for Tuberculosis Control and Prevention, Chinese Center for Disease Control and Prevention, Beijing, China

<sup>3</sup>Department of Veterinary Medicine, College of Animal Sciences, Zhejiang University, Hangzhou, China

## Correspondence

Houhui Song, College of Animal Science and Technology, College of Veterinary Medicine, Key Laboratory of Applied Technology on Green-Eco-Healthy Animal Husbandry of Zhejiang Province, Zhejiang Provincial Engineering Laboratory for Animal Health Inspection and Internet Technology, Zhejiang A&F University, Hangzhou 311300, Zhejiang, China.  
Email: songhh@zafu.edu.cn

## Funding information

National Natural Science Foundation of China (NSFC), Grant/Award Number: 31502034, 31502127, 31802258, 31802258, 31902249, 31602119, 31602062, 31502127, 31770040 and 31972648; Natural Science Foundation of Zhejiang Province (Zhejiang Provincial Natural Science Foundation), Grant/Award Number: LQ15C180002, LQ19C180003, LQ20C180002 and LZ19C180001; the key Research and Development Program of Zhejiang Province, Grant/Award Number: 2019C02043; ZAFU talents starting program, Grant/Award Number: 2014FR069

## Abstract

Pathogenic mycobacteria, such as *Mycobacterium tuberculosis*, *Mycobacterium bovis*, and *Mycobacterium marinum*, can trigger NLRP3 inflammasome activation leading to maturation and secretion of interleukin 1 $\beta$  (IL-1 $\beta$ ). However, the mycobacterial factors involved in the activation of NLRP3 inflammasome are not fully understood. Here, we identified that the PPE family protein PPE13 was responsible for the induction of IL-1 $\beta$  secretion in a NLRP3 inflammasome-dependent manner. We found that the recombinant *Mycobacterium smegmatis* expressing PPE13 activates NLRP3 inflammasome, thereby inducing caspase-1 cleavage and IL-1 $\beta$  secretion in J774A.1, BMDMs, and THP-1 macrophages. To examine whether this inflammasome activation was triggered by PPE13 rather than components of *M. smegmatis*, PPE13 was introduced into the aforementioned macrophages by lentivirus as a delivery vector. Similarly, this led to the activation of NLRP3 inflammasome, indicating that PPE13 is a direct activator of NLRP3 cascade. We further demonstrated that the NLRP3 complex activated the inflammasome cascade, and the assembly of this complex was facilitated by PPE13 through interacting with the LRR and NATCH domains of NLRP3. Finally, we found that all PPE13 proteins isolated from *M. tuberculosis*, *M. bovis*, and *M. marinum* can activate NLRP3 inflammasome through binding to NLRP3, which requires C-terminal repetitive MPTR domain of PPE13. Thus, we, for the first time, revealed that PPE13 triggers the inflammasome-response by interacting with the MPTR domain of PPE13 and the LRR and NATCH domains

**Abbreviations:** AIM2, absent in melanoma 2; ASC, apoptosis-associated speck-like protein containing a CARD; BMDM, bone marrow-derived macrophage; EXS, 6-kDa early secretory antigenic target (ESAT-6) secretion system; IL-1 $\beta$ , interleukin 1 $\beta$ ; IL-6, interleukin 6; IL-10, interleukin 10; LDH, lactate dehydrogenase; LPS, lipopolysaccharides; NEK7, NIMA-related kinase 7; Nig, Nigericin; NLRP3, NACHT, LRR, and PYD domains-containing protein 3; TNF- $\alpha$ , tumor necrosis factor- $\alpha$ .

Yang Yang and Pianpian Xu contributed equally to this work.

of NLRP3. These findings provide a novel perspective on the function of PPE proteins in the immune system during mycobacteria invasion.

#### KEYWORDS

IL-1 $\beta$ , mycobacteria, NLRP3 inflammasome, PPE13

## 1 | INTRODUCTION

Tuberculosis (TB) is a major cause of morbidity and mortality worldwide. It is caused by *Mycobacterium tuberculosis* (*M. tuberculosis*) and/or *Mycobacterium bovis* (*M. bovis*). In 2017, an estimated 10 million TB cases and 1.3 million TB deaths were recorded.<sup>1</sup> Pathogenic mycobacteria primarily infect host macrophages and elicit the secretion of several cytokines that influence the outcome of mycobacteria infection.<sup>2</sup>

The pro-inflammatory cytokine interleukin-1 $\beta$  (IL-1 $\beta$ ) is considered to play an important role in host resistance to mycobacteria infection.<sup>3-7</sup> Mice deficient in IL-1 $\beta$  are more susceptible to *M. tuberculosis* and exhibit increased mortality and bacterial burden in the lung.<sup>7</sup> Treatment of *M. tuberculosis*-infected macrophages with exogenous IL-1 $\beta$  reduced bacterial burden through the induction of eicosanoids.<sup>8</sup> The expression and processing of IL-1 $\beta$  is tightly regulated by inflammasomes.<sup>9</sup> Previous studies have shown that pathogenic mycobacteria, such as *M. tuberculosis*, *M. bovis*, and *Mycobacterium marinum* (*M. marinum*), can trigger AIM2<sup>10,11</sup> and NLRP3 inflammasomes activation.<sup>12-14</sup> This promotes IL-1 $\beta$  release, which requires type VII secretion system ESX-1 and its substrate. ESAT-6 is an ESX-1 substrate which has been identified to facilitate NLRP3 inflammasome activation.<sup>15</sup> However, ESX-1 mutant does not completely abolish the secretion of IL-1 $\beta$  during mycobacteria infection. Moreover, infection of the attenuated mycobacteria strain H37Ra, which is defective for secretion of ESAT-6, still leads to high secretion of IL-1 $\beta$ .<sup>16</sup> This implies that other unknown mechanisms or factors of mycobacteria may regulate the secretion of IL-1 $\beta$  secretion through inflammasomes.

Abdallah et al and Swati et al found that ESX-5 mutant strains of *M. tuberculosis* and *M. marinum* do not induce IL-1 $\beta$  secretion, although ESAT-6 secretion is not affected in ESX-5 mutant.<sup>17-19</sup> ESX-5 substrates might be involved in the regulation of IL-1 $\beta$  secretion through a mechanism different from that of ESX-1-induced IL-1 $\beta$  secretion. ESX-5 is known to fine-tune the secretion of PE and PPE proteins,<sup>20</sup> which are characterized by a conserved N-terminal domain with Pro-Glu (PE) and Pro-Pro-Glu (PPE).<sup>21</sup> Since the PPE domain is highly conserved in all members of PPE family, it suggested that all PPE proteins may share same cellular localization and several studies have shown that PPE proteins were found associated with the mycobacterial cell wall.<sup>20,22-24</sup> Moreover, based on the presence of characteristic

motifs in C-terminal domains, PE and PPE families are divided into two and four subfamilies, respectively.<sup>25</sup> The PPE\_MPTR (major polymorphic tandem repeat) subfamily, the second largest group in PPE family, is characterized by containing multiple C-terminal repeats of motif NxGxNxG.<sup>26</sup> Emerging data suggested that PPE\_MPTR might be involved in the virulence of mycobacteria, since most of the viability in *M. tuberculosis* clinical isolates rests on PPE\_MPTR and PE\_PGRS.<sup>27</sup> A previous study showed that PPE13, as a member of PPE\_MPTR protein, was upregulated in the lung specifically during chronic infection with mycobacteria.<sup>28</sup> In addition, PPE13 has been reported to be involved in mycobacterial survival in macrophages.<sup>29</sup> However, the exact function of PPE13 in mycobacteria pathogenesis remains poorly understand. Here, we reveal that PPE13 promotes cell death and IL-1 $\beta$  secretion in a NLRP3 inflammasome-dependent manner. Mechanistically, we show that PPE13 directly interacts with LRR and NACHT domains of NLRP3 to trigger the NLRP3 complex assembly and its activation. Further, we confirm that three PPE13 proteins isolated from *M. bovis*, *M. tuberculosis*, and *M. marinum* activates NLRP3 inflammasome and binds to NLRP3 through its MPTR domain.

## 2 | MATERIALS AND METHODS

### 2.1 | Antibodies and reagents

Anti-IL-1 $\beta$  (#12703), anti-cleaved IL-1 $\beta$  (#83185), anti-ASC (#67824), and anti-HA (#3724) were purchased from cell signaling technology. LPS (O11:B4, L2630), Anti-Flag M2 (F1804), anti-c-Myc (M5546), and anti-GAPDH (G9545) were purchased from Sigma-Aldrich. Anti-Caspase-1(p20) antibody (AG-20B-0042) was purchased from AdipoGen. Rabbit anti-GroEL2 polyclonal antibody was generated by immunization with prokaryotic purified GroEL2. Secondary HRP-conjugated goat anti-rabbit IgG (#7074) and goat anti-mouse IgG (#7076) were purchased from cell signaling technology. Fluorescein isothiocyanate-conjugated goat anti-rabbit IgG (Alexa Fluor 488, ab150077), goat anti-mouse IgG (Chrome 546, ab60316), and donkey anti-rabbit IgG (Alexa Fluor 647, ab150075) were purchased from Abcam. Caspase-1 specific inhibitor z-YVAD-fmk (A8955) and NLRP3 inhibitor MCC950 (C3780) were purchased from Apexbio. Murine M-CSF (315-02) was from PeproTech. ATP (tlrl-atpl) and Nigericin (tlrl-nig) were from InvivoGen.

## 2.2 | Construction of recombinant *M. smegmatis* strains expressing PPE13 protein

The full-length gene of PPE13 (Mb0902c) with a C-terminal HA-tag was amplified from the genomic DNA of *M. bovis* Beijing strain using specific primers (forward primer, 5'-CGAGTTAATTAAGAAAGGAGGTTAATAATGAATTCATGGTG. CTGCCGCC-3' and reverse primer, 5'-GAAGAAGCTTTTAAGCGTAATCTGGAA. CATCGTATGGGTACTTTTTTTGGGGGGGGGCA-3'). The PCR products were cloned between the *Pac* I and *Hind* III sites of pMS2 expression vector. The pMS2-*ppe13* plasmid was then electroporated into *M. smegmatis* mc<sup>2</sup>155 to generate recombinant *M. smegmatis* (Ms\_PPE13). Expression of PPE13 was confirmed by Western blot using anti-HA-tag antibody (cell signaling technology). *M. smegmatis* transformed with pMS2 vector (Ms\_Vec) was used as control group.

## 2.3 | Subcellular fractionation of recombinant *M. smegmatis*

The Ms\_PPE13 and Ms\_Vec were cultured and subjected to subcellular fractionation separation as described previously.<sup>30</sup> Generally, Ms\_PPE13 and Ms\_Vec were grown overnight in a 50 mL culture of 7H9/Tween-80/Hyg at 37°C with shaking at 200 rpm. Bacteria were then harvested by centrifugation at 5000 ×g for 10 minutes. The pellets were resuspended in 2 mL of PBS buffer and sonicated with 10 × 10 s pulses. The whole lysates were centrifuged at 4°C to remove cell debris. The supernatants were then removed and centrifuged at 27 000 ×g for 30 minutes to obtain the cell wall pellet. The remaining supernatants were cell membrane and cytosol fractions. Samples from each of fractions were subjected to western blot using anti-HA antibody (cell signaling technology). GroEL2 protein, served as cytosol marker protein of mycobacteria, was detected by anti-GroEL2 polyclonal antibody (1:10 000 in dilution).

## 2.4 | Bacterial strains and growth conditions

Recombinant *M. smegmatis* strain Ms\_PPE13 was generated to express PPE13 protein of *M. bovis*. Another recombinant strain Ms\_Vec harboring the backbone vector was constructed as the control. The detailed procedures for constructing Ms\_Vec and Ms\_PPE13 are described in the Supplementary Materials and Methods. Mycobacterial strains were grown in Middlebrook 7H9 broth medium supplemented with 0.05% of Tween-80, 0.5% of glycerol, and 50 µg/mL of hygromycin B.

## 2.5 | Cell culture

Mouse J774A.1 and human HEK293T were cultured in Dulbecco's modified Eagle's medium (DMEM) supplemented with 10% of fetal bovine serum (FBS), 100 mg/mL of streptomycin, and 100 U/mL of penicillin. Human THP1-KO-NLRP3 cells were knockout of NLRP3 gene in THP-1 cells and purchased from InvivoGen (thp-konlrp3). Human THP-1 and THP1-KO-NLRP3 cell line were cultured in PRIM 1640 medium containing 10% of FBS, 100 mg/mL of streptomycin, and 100 U/mL of penicillin. Mouse bone marrow-derived macrophage (BMDM) cells were isolated from femurs of female 6-8-week-old C57BL/6 mice as described previously<sup>11</sup> and differentiated for 7 days in RPMI 1640 medium containing 10% of FBS, 10 ng/mL of M-CSF, 100 microgram/ml of streptomycin, and 100 U/mL of penicillin. Cells were maintained in an incubator at 37°C with 5% of CO<sub>2</sub>.

## 2.6 | Macrophage infection with recombinant *M. smegmatis* strains

J774A.1 and BMDMs cells were seeded at a density of 3 × 10<sup>5</sup> cells per well in 24-well plates. THP-1 cells were seeded in 24-well plates at a density of 2 × 10<sup>5</sup> cells per well. To differentiate into macrophages, THP-1 cells were exposed to 100 ng/mL phorbol 12-myristate 13-acetate (PMA, Sigma Aldrich) for 24 hours, and then cultured for another 24 hours without PMA. Thereafter, macrophages were infected with Ms\_Vec or Ms\_PPE13 at MOI of 10. After 4 hours of infection, the infected cells were washed with PBS three times and incubated for additional 2 hours in DMEM or RPMI 1640 medium supplemented with 100 µg/mL gentamicin to remove extracellular bacteria.

## 2.7 | Lactate dehydrogenase (LDH) assay

J774A.1 were seeded at a density of 50 000 cells per well in 96-well plates and infected with *M. smegmatis* as described above. Supernatants were collected and subjected to LDH activity assay using CytoTox 96 LDH-release assay kit (Promega).

## 2.8 | RNA extraction and quantitative RT-PCR

Total RNA was extracted from the samples using EASYspin tissue/cell RNA isolation kit (Aialab Biotechnologies Co) according to the manufacturer's instructions. Reverse transcription of 1 µg total RNA was carried out to synthesize

cDNA using reverse transcriptase (Toyobo). qRT-PCR was performed using SYBR green PCR master mix (Takara). Relative mRNA levels were calculated by the  $2^{-\Delta\Delta Ct}$  method and are shown as relative fold changes. Primers used for qRT-PCR are listed in Supplementary Table S1.

## 2.9 | ELISA

Levels of interleukin (IL)-1 $\beta$ , tumor necrosis factor (TNF)- $\alpha$ , IL-6, and IL-10 in supernatants were measured by ELISA kits (MultiSciences) according to the manufacturer's instructions. Levels of cleaved caspase-1 in supernatants were measured by ELISA kits (InvivoGen) according to the manufacturer's instructions.

## 2.10 | Western blot analysis

Cell lysates were prepared by treatment with Radio immunoprecipitation assay (RIPA) buffer, and then mixed with 4 $\times$  SDS sample buffer at 100 $^{\circ}$ C for 10 minutes. To detect mature IL-1 $\beta$ , the culture supernatant was concentrated using Amicon Ultra-0.5 mL Centrifugal Filters (C82301, Millipore). The protein samples were separated by 10%-15% of SDS-PAGE gels and transferred onto PVDF membrane. Membranes were incubated with antibodies and developed using ECL substrate (Bio-Rad).

## 2.11 | Plasmid construction and lentivirus production

The fragments of mouse NLRP3 (NM\_145827.3), ASC (NM\_023258.4), Caspase-1 (NM\_009807.2), NEK7 (NM\_021605.4), LRR, NBD, and PYD were obtained by RT-PCR from J774A.1 cells and cloned into pCMV-Myc or p3  $\times$  Flag-CMV-7.1 vectors. The fragments of mouse IL-1 $\beta$  (NM\_008361.4) was cloned into pEGFP-C1 vector. The full length of PPE13, PPE domain, and MPTR domain were amplified by PCR from genomic DNA of *M. bovis* Beijing strain using specific primers and cloned into the site of *EcoR* I and *Xho* I of pCMV-Myc or pCMV-HA vector. The fragments of PPE13 amplified from *M. tuberculosis* (Rv0878c) or *M. marinum* (MMAR\_4319) genomic DNA were cloned into pCMV-Myc vector. Primers used for plasmid construction are listed in Supplementary Table S2.

To construct a lentivirus expressing PPE13 from *M. bovis*, a fragment of PPE13 was cloned into pHBIV-CMV-EF1-GFP vector, and transfected into HEK293T cells together with psPAX2 and pMD2.G using lipofectamine 2000. After 48 hours of transfection, supernatants were harvested,

centrifuged at 1000  $\times$ g for 10 minutes, and filtered through 0.45  $\mu$ m filters. THP-1 cells were infected with the supernatants containing lentiviral particles in the presence of 6  $\mu$ g/mL of polybrene (Sigma). Culture supernatants were collected 24 hours after infection and used to measure IL-1 $\beta$  secretion by ELISA kit. To establish a THP-1 cell line stably expressing PPE13, cells were selected by 1.5  $\mu$ g/mL of puromycin (Sigma) after 72 hours of culture.

## 2.12 | Coimmunoprecipitation assay

After 24 hours of transfection, HEK293T cells were lysed with lysis buffer containing 50 mM of Tris (pH7.4), 150 mM of NaCl, 2 mM of EDTA, 10% of glycerol, and 1% of NP-40, supplemented with a protease inhibitor cocktail (#5871, CST). Lysates were incubated overnight at 4 $^{\circ}$ C with anti-flag M2 affinity gel (A2220, Sigma Aldrich) or mouse immunoglobulin G antibody (mouse (G3A1) mAb IgG1 isotype, 5415, CST) plus Protein-A Sepharose (P9424, Sigma Aldrich). The beads were washed five times with lysis buffer and the immunoprecipitated were eluted with SDS loading buffer and subjected to western blot assay.

## 2.13 | ASC oligomerization detection

HEK293T cells were seeded at a density of  $1 \times 10^6$  cells per well in 6-well tissue culture plates and transfected with appropriate plasmids. After 24 hours of transfection, cells were lysed with ice-cold buffer A containing 20 mM of HEPES-KOH (pH 7.5), 10 mM of KCl, 1.5 mM of MgCl $_2$ , 1 mM of EDTA, 1 mM of EGTA, and 320 mM of sucrose. Lysates were centrifuged at 6000  $\times$ g for 15 minutes. Pellets were washed twice with PBS, resuspended in PBS and cross-linked using fresh disuccinimidyl suberate (DSS, 2 mM, Sigma Aldrich) at 37 $^{\circ}$ C for 30 minutes. The cross-linked pellets were centrifuged and resuspended in SDS loading buffer for western blot assay.

## 2.14 | Confocal microscopy

BMDMs (for ASC specks detection) or HEK293T cells (for co-localization detection) were plated at a density of  $1 \times 10^5$  cells per well overnight on coverslips and infected or transfected as described above. Cells were fixed in 4% of paraformaldehyde at RT for 30 minutes following by incubation with appropriate antibodies and DAPI (4',6-diamidino-2-phenylindole; Thermo Fisher Scientific) staining. The stained cells were examined under a laser scanning microscope (Zeiss LSM510 META, Zeiss Germany).

## 2.15 | Statistical analysis

All assays were performed at least three times independently. Data are presented as mean  $\pm$  SD and analyzed using two-tailed Student's *t* test, one-way ANOVA or two-way ANOVA followed by Tukey's multiple comparisons test by Prism software (GraphPad). The differences were considered significant when  $P < .05$  (\*),  $P < .01$  (\*\*), and  $P < .001$  (\*\*\*)

## 3 | RESULTS

### 3.1 | PPE13 induces cell death and IL-1 $\beta$ secretion in macrophages

Given that the nonpathogenic, fast-growing *M. smegmatis* does not contain a PPE13 orthologous,<sup>31</sup> we generated the recombinant *M. smegmatis* strain expressing a HA-tagged PPE13 protein (named as Ms\_PPE13) from *M. bovis* (Supplementary Figure 1A) to investigate the role of PPE13 in pathogenicity of mycobacterial infection. We examined the effect of PPE13 on cytotoxicity of *M. smegmatis* by measuring release of LDH from J774A.1 cells infected with Ms\_PPE13. Levels of cell death in macrophages infected

with Ms\_PPE13 were more than levels seen in macrophages infected with Ms\_Vec at 24 and 48 hours postinfection (Figure 1A). To confirm the physiological relevance of this finding, BMDMs and PMA-differentiated THP-1 cells were treated with Ms\_PPE13. We observed that Ms\_PPE13 induced a high level of cell death at 48 hours postinfection (Figure 1D and Supplementary Figure 2). These results suggested that PPE13 induces cell death during *M. smegmatis* infection.

Next, we examined whether PPE13 affects inflammatory cytokines production during mycobacterial infection. Notably, PPE13 significantly enhanced both IL-1 $\beta$  mRNA production and protein secretion (Figure 1B,C). PPE13 induced greater relative increase in IL-6 mRNA, but much less difference in protein level was observed between Ms\_PPE13 and Ms\_Vec groups (Supplementary Figure 3A,B). In addition, PPE13 did not affect the release of TNF- $\alpha$  and IL-10 into supernatants (Supplementary Figure 3C-F). Moreover, the increase of IL-1 $\beta$  secretion upon infection with Ms\_PPE13 was also observed in BMDMs at 24 and 48 hours postinfection (Figure 1E). In addition, Ms\_PPE13 induced more mature IL-1 $\beta$  secretion in PMA-differentiated THP-1 cells at 6 and 24 hours postinfection (Supplementary Figure 4A). These results demonstrated that PPE13 induces IL-1 $\beta$  secretion from macrophages during infection with *M. smegmatis*.

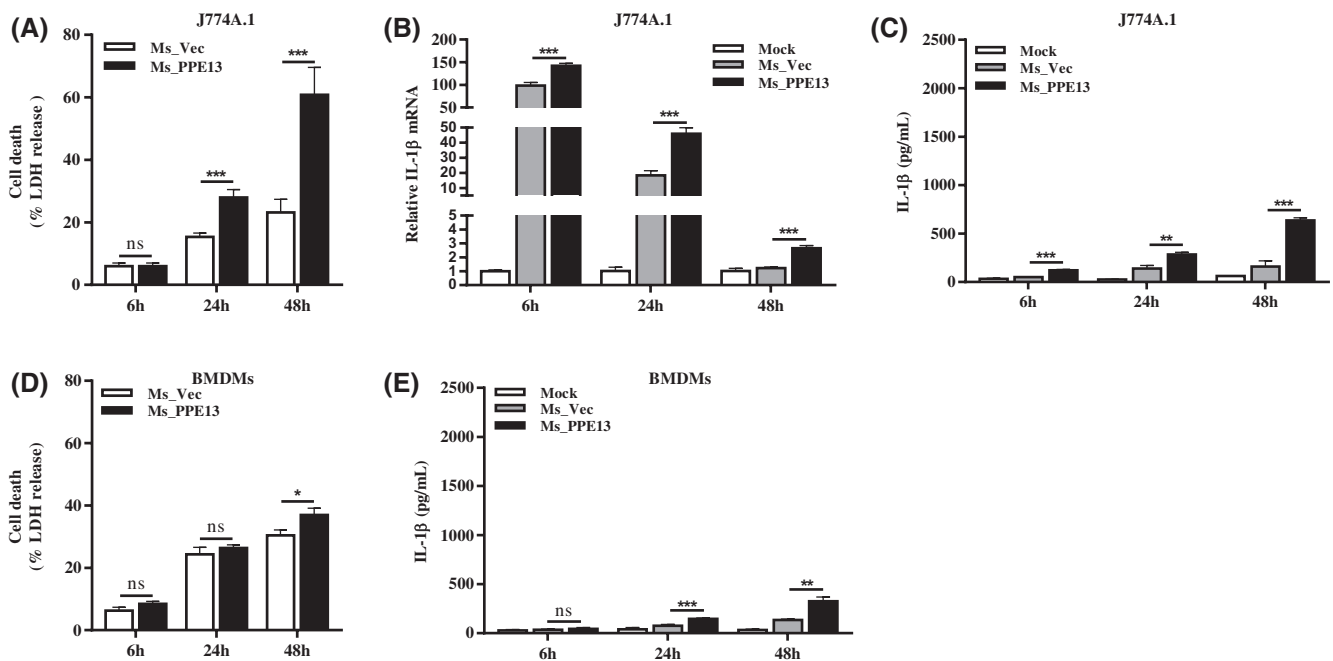


**FIGURE 1** PPE13 induces cell death and IL-1 $\beta$  secretion in mouse macrophages during infection with *M. smegmatis*. A-C, J774A.1 cells were infected with Ms\_Vec or Ms\_PPE13 at MOI of 10 for 6, 24, or 48 hours. A, Percentages of cell death were analyzed by detecting LDH release into supernatants. B, Transcriptional expressions of *IL-1 $\beta$*  were quantified by RT-PCR. C, IL-1 $\beta$  secretion into supernatants were detected by ELISA. D and E, BMDM cells were infected with Ms\_Vec or Ms\_PPE13 at MOI of 10 for 6, 24, or 48 hours. D, Percentages of cell death were analyzed by detecting LDH release into supernatants. E, IL-1 $\beta$  secretion into supernatants was analyzed by ELISA. Data are representative of three independent experiments. Values are mean  $\pm$  SD, \* $P < .05$ , \*\* $P < .01$ , \*\*\* $P < .001$  and ns = nonsignificant

### 3.2 | PPE13-induced IL-1 $\beta$ secretion is dependent on the NLRP3 inflammasome activation

The processing of IL-1 $\beta$  secretion requires two steps: first, IL-1 $\beta$  is synthesized as inactive precursor pro-IL-1 $\beta$ , which is regulated by NF- $\kappa$ B activation; second, pro-IL-1 $\beta$  is cleaved and by caspase-1 into mature and active form.<sup>32</sup> Given that PPE13 upregulates the transcript level of IL-1 $\beta$ , we used cycloheximide (CHX, a translation inhibitor) to investigate whether PPE13 induces IL-1 $\beta$  secretion mainly via translation. The results showed that, even with blocking new translation of pro-IL-1 $\beta$ , Ms\_PPE13 induced more release of IL-1 $\beta$  compared to Ms\_Vec (Figure 2A), indicating that Ms\_PPE13 is inducing release of IL-1 $\beta$  in a translation-independent manner. Next, we examined whether PPE13 affect the activation of caspase-1. In ELISA and western blot assays, Ms\_PPE13 increased cleavage of caspase-1 in BMDMs as compared to Ms\_Vec (Figure 2B). Furthermore, treatment with caspase-1 specific inhibitor z-VYAD-fmk significantly reduced IL-1 $\beta$  secretion in BMDMs infected with Ms\_PPE13 (Figure 2C). These data sets suggested that the effect of PPE13 on IL-1 $\beta$  secretion is dependent on caspase-1 activation.

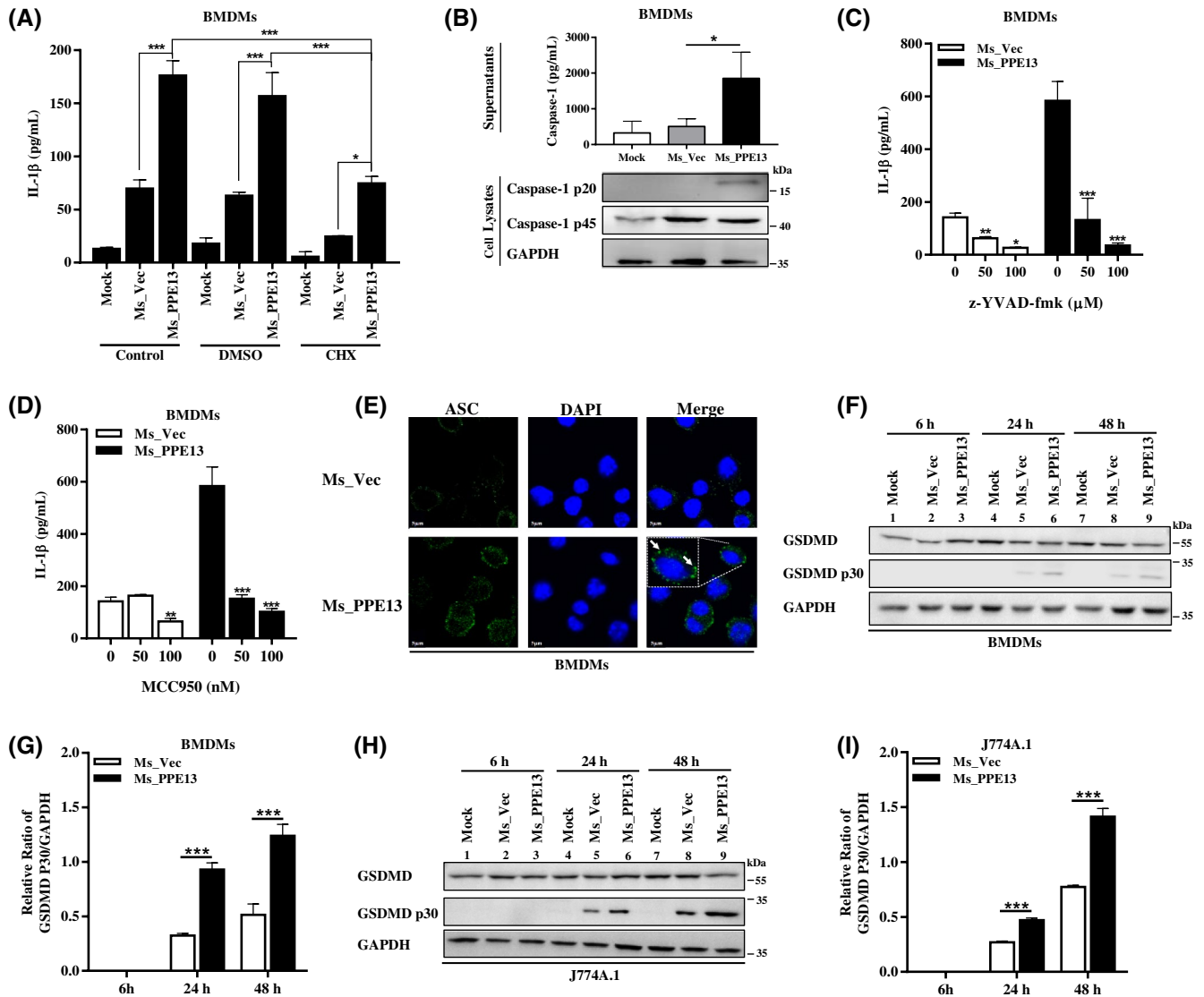
Previous studies demonstrated that mycobacterial infection triggers caspase-1 activation via AIM2 and NLRP3 inflammasomes.<sup>10,11,15</sup> Given that AIM2 is a double-strand DNA sensor, we hypothesized that PPE13 may possibly mediate the autocatalysis of caspase-1 and subsequent IL-1 $\beta$  secretion by activating NLRP3 inflammasome. To test this hypothesis, macrophages were treated with MCC950, a NLRP3 inflammasome specific inhibitor,<sup>33</sup> during infection with recombinant *M. smegmatis* strains. The results showed that IL-1 $\beta$  secretion was attenuated by MCC950 in a dose-dependent manner (Figure 2D). In addition, NLRP3 deficient THP-1 cells exhibited a decrease in PPE13-induced IL-1 $\beta$  secretion as compared to wild-type cells (Supplementary Figure 4B). ASC oligomerization is a critical step in NLRP3 inflammasome complex formation.<sup>32</sup> Immunofluorescence analysis showed that Ms\_PPE13 infection produced a higher percentage of ASC-specks, suggesting that PPE13 facilitates ASC oligomerization (Figure 2E). Moreover, pyroptosis is dependent on NLRP3 inflammasome. Caspase-1 also cleave the cytosolic protein gasdermin D (GSDMD) into p30 to form plasma membrane pores and subsequently rupture plasma membrane, resulting in the release of cytosolic LDH into the extracellular space. Given that PPE13 could induce cell death by measurement the release of LDH as showed above, we detected the effect of PPE13 on pyroptosis by measuring the cleavage of GSDMD both in J774A.1 (Figure 2H,I), BMDMs (Figure 2F,G), and THP-1 cells (Supplementary

Figure 4C,D). As shown, compared to Ms\_Vec, Ms\_PPE13 can cleave more full length of GSDMD to produce GSDMD-NT (p30) as compared to Ms\_Vec. Overall, these results indicated that PPE13 activates the NLRP3 inflammasome, resulting in caspase-1 activation, subsequent IL-1 $\beta$  secretion, and GSDMD-mediated pyroptosis.

### 3.3 | PPE13 directly triggers the activation of NLRP3 inflammasome

Subcellular fractionation analysis showed that PPE13 was located on the cell wall (Supplementary Figure 1B). Thus, we explored whether PPE13 has a direct role in NLRP3 inflammasome activation process. THP-1 cells were infected with lentivirus expressing PPE13 and the ability of PPE13 to drive NLRP3 inflammasome activation was determined by measuring the level of IL-1 $\beta$  in comparison with cells exposed to lentivirus containing empty vector. The results revealed that PPE13 enhanced IL-1 $\beta$  secretion at 24 and 48 hours postinfection (Figure 3A). Interestingly, this effect was abolished by z-YVAD-fmk and MCC950 (Figure 3B,C). To further confirm the effect of PPE13 on NLRP3 inflammasome activation, we constructed a THP-1 cell line stably expressing PPE13. LPS treatment alone could increase IL-1 $\beta$  secretion in this cell line. Furthermore, LPS + Nig/ATP treatment significantly increased IL-1 $\beta$  production in THP-1 stably expressing PPE13 compared to WT THP-1 (Figure 3D).

To demonstrate the direct interaction between PPE13 and NLRP3 inflammasome, we reconstituted an in vitro NLRP3 inflammasome system in HEK293T cells, in which the NLRP3 inflammasome is absent. As shown in Figure 3E, co-transfection of PPE13 and the components of NLRP3 complex significantly promoted IL-1 $\beta$  secretion in a dose-dependent manner. Upon activation, NLRP3 undergoes a conformational change and interacts with ASC to form an active inflammasome complex. We tested whether PPE13 could affect NLRP3-ASC interaction. HEK293T cells were transfected with NLRP3 and ASC with or without PPE13, and then, co-immunoprecipitation assays for NLRP3 was performed. It was found that PPE13 enhanced the interaction between NLRP3 and ASC (Figure 3F). ASC oligomerization is considered to be a key event in caspase-1 activation and inflammasome function. Thus, we assessed the effect of PPE13 on ASC oligomerization in HEK293T cells. When ASC and PPE13 were co-expressed in HEK293T cells, ASC oligomerization was not affected; however, when ASC, NLRP3, and PPE13 were co-expressed, ASC oligomerization was enhanced (Figure 3G). Collectively, these results suggested that PPE13 facilitates ASC oligomerization through NLRP3.



**FIGURE 2** PPE13-induced IL-1 $\beta$  secretion is required for NLRP3 inflammasome. A, BMDMs were pretreated with or without 5  $\mu$ g/mL CHX for 2 hours, and then, infected with Ms\_Vec or Ms\_PPE13 at MOI of 10. Supernatants were collected to determine IL-1 $\beta$  levels by ELISA. Data were analyzed by two-way ANOVA followed by Tukey's multiple comparisons test. B, BMDMs were infected with Ms\_Vec or Ms\_PPE13 at MOI of 10 for 48 hours. Levels of caspase-1 in supernatants were determined by ELISA (upper panel). Levels of cleaved caspase-1 (p20), pro-caspase-1 (p45), or GAPDH in cell lysates were detected by western blot (lower panel). C and D, BMDMs were pretreated with or without z-YVAD-fmk (50 or 100  $\mu$ M) or MCC950 (50 or 100 nM) for 1 hours, and then, infected with Ms\_Vec or Ms\_PPE13 at MOI of 10 for 48 hours in the presence or absence of z-YVAD-fmk (C) or MCC950 (D). Supernatants were collected to determine IL-1 $\beta$  levels by ELISA. E, ASC specks formation (green) was observed by confocal microscopy in BMDMs infected with Ms\_PPE13 or Ms\_Vec at MOI of 10 for 48 hours. Nuclei were stained with DAPI. Scale bar is 5  $\mu$ m. F and H, Cleavage of GSDMD was detected by western blot in BMDMs (F) and J774a.1 (H) infected with Ms\_PPE13 or Ms\_Vec. G and I, The relative densities of the expression of GSDMD p30 were analyzed by densitometry. Data are representative of three independent experiments. Values are mean  $\pm$  SD, \* $P < .05$ , \*\* $P < .01$ , \*\*\* $P < .001$

### 3.4 | PPE13 binds to NLRP3 through NACHT and LRR domains to promote NLRP3 inflammasome assembly

To further elucidate the underlying mechanism by which PPE13 facilitates NLRP3 inflammasome activation, experiments were carried out to determine whether PPE13 interacts with the components of NLRP3 inflammasome. HEK293T cells were transfected with PPE13 along with

NLRP3, ASC, or caspase-1, and then, subjected to co-immunoprecipitation assays. The results revealed that PPE13 interacted with NLRP3 but not with ASC and caspase-1 (Figure 4A). Immunoprecipitation of Flag-tagged PPE13 demonstrated the interaction of Myc-tagged NLRP3, and the same was true of the reciprocal experiment using immunoprecipitation of Myc-tagged NLRP3 (Figure 4B). Furthermore, in THP-1 cells stably expressing PPE13, PPE13 also interacted with endogenous NLRP3

(Supplementary Figure 5A). These results indicated that PPE13 can bind to NLRP3.

To further examine the details of this interaction, the interaction of PPE with functional domains in NLRP3 was mapped. NLRP3 contains three domains, namely, PYD, NACHT (nucleotide binding domain or NBD), and LRR domains. Co-immunoprecipitation assays showed that PPE13 interacted with NLRP3, NACHT (91-710 aa), and LRR

(711-1033 aa), but not with PYD (1-90 aa) (Figure 4C). PPE13 also co-localized with NACHT and LRR domains (Figure 4D). We also confirmed the relationships between PPE13 and NLRP3 in human origin. PPE13 also interacted with human-original NLRP3 through NACHT and LRR domains (Supplementary Figure 5B). Taken together, these results demonstrated that PPE13 binds to NLRP3 by interacting with NACHT and LRR domains.

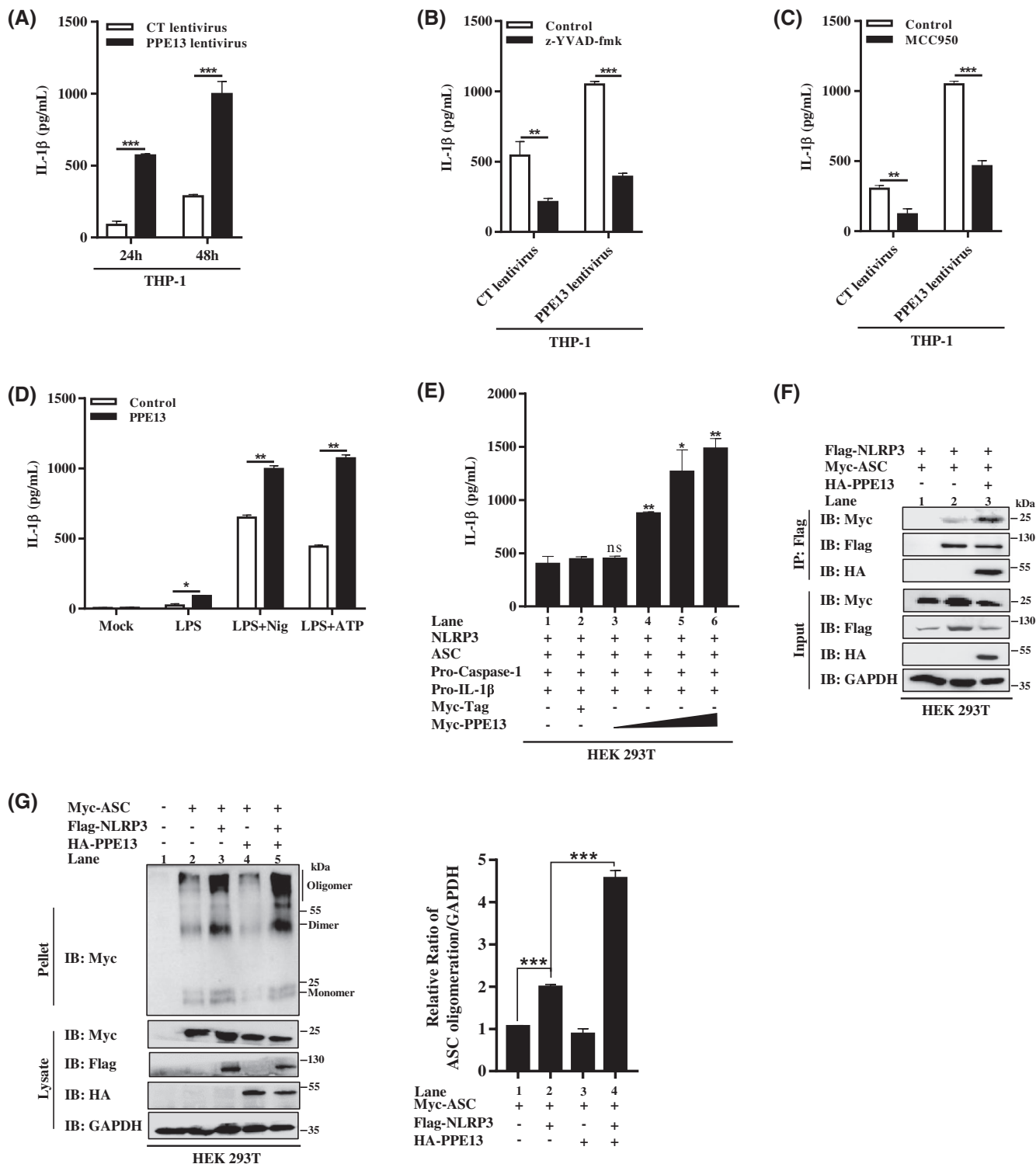




**FIGURE 3** PPE13 has a direct role in the activation of NLRP3 inflammasome. A, The PMA-differentiated THP-1 cells were infected with lentivirus containing an empty vector (named as CT lentivirus) or lentivirus expressing PPE13 (named as PPE13 lentivirus) for 24 or 48 hours. Supernatants were collected and analyzed for IL-1 $\beta$  by ELISA. B, The PMA-differentiated THP-1 cells were infected with CT-lentivirus or PPE13 lentivirus for 24 hours in the presence or absence of z-YVAD-fmk (100  $\mu$ M) or C, MCC950 (10  $\mu$ M). D, THP-1 cells stably expressing PPE13 were treated with LPS (1  $\mu$ g/mL), LPS + Nig (10  $\mu$ M), LPS + ATP (5 mM), respectively. E, HEK293T cells were transfected with plasmids encoding NLRP3, ASC, pro-Casp-1, pro-IL-1 $\beta$  together with myc-tag (myc tagged empty vector, 400 ng) or increasing amount of myc-PPE13 (100, 200, 300, and 400 ng). F, HEK293T cells were co-transfected with Flag-NLRP3, Myc-ASC, or HA-PPE13. A specific amount of cell lysates (appropriately 30  $\mu$ g) was subjected to western blot using anti-Flag, anti-Myc, anti-HA, and anti-GAPDH antibodies (Input, lower panel). The remaining part of cell lysates was immunoprecipitated with anti-Flag antibody or control mouse immunoglobulin G (IgG), and then, analyzed with anti-Flag, anti-Myc, and anti-HA antibodies by western blot (IP, upper panel). G, HEK293T cells were transfected with Myc-ASC together with HA-Tag (an empty vector), Flag-NLRP3, or HA-PPE13. Cell lysates were centrifuged to form pellets, which were subjected to ASC oligomerization assay and analyzed by western blot using anti-Myc antibody. The relative densities of ASC oligomerization were analyzed by densitometry. Data are representative of three independent experiments. Values are mean  $\pm$  SD, \* $P$  < .05, \*\* $P$  < .01, \*\*\* $P$  < .001

We next examined the effect of PPE13 on NLRP3 inflammasome assembly. NLRP3 oligomerization through NACHT domain is a critical event for NLRP3 inflammasome assembly and ASC recruitment. We then determined whether PPE13 could promote NLRP3-NLRP3 interaction. Indeed, PPE13 significantly enhanced the interaction of Myc-tagged NLRP3 and HA-tagged NLRP3 in transfected HEK293T cells (Figure 4F). PPE13 could also promote NLRP3 interaction with NEK7, a newly identified NLRP3 components (Figure 4G). However, PPE13 had no effect on caspase-1 and ASC interaction (Figure 4H). Together, these data suggested that PPE13 can bind to NLRP3 through NACHT and LRR domains to promote NLRP3 inflammasome assembly.

### 3.5 | MPTR domain of PPE13 binds to NLRP3 to induce IL-1 $\beta$ secretion

*M. bovis*, *M. tuberculosis*, and *M. marinum* have been recognized to stimulate NLRP3 inflammasome activation.<sup>12-14</sup> Thus, we investigated whether PPE13 isolated from *M. tuberculosis* and *M. marinum* could interact with NLRP3. HEK293T cells were transfected with NLRP3 together with Mb\_PPE13, Mtb\_PPE13, or Mm\_PPE13, and then, subjected to co-immunoprecipitation assays. We found that all PPE13 proteins from different strains interacted with NLRP3 (Figure 5A). Moreover, the effects of three PPE13 proteins on the activation of NLRP3 inflammasome were determined. HEK293T cells were co-transfected together with the components of NLRP3 complex, and then, transfected with each of PPE13 from different strains, respectively. Similar to Mb\_PPE13, Mtb\_PPE13, and Mm\_PPE13 enhanced IL-1 $\beta$  secretion into the cell supernatants (Figure 5B).

PPE13 contains a conserved N-terminal domain with Pro-Pro-Glu (named as PPE domain) and a C-terminal domain with multiple repeats of motif NxGxNxG (named as MPTR domain).<sup>26</sup> To investigate the domains of PPE13 involved in NLRP3 interaction, two plasmids containing PPE domain (1-180 aa) and MPTR domain (165-438 aa) were constructed. Co-immunoprecipitation assays showed that NLRP3 interacts

with PPE13 and MPTR domain, but not with PPE domain (Figure 5C). Confocal microscopy revealed that NLRP3 and MPTR domain were co-localized (Figure 5D). In addition, MPTR domain, but not PPE domain, enhanced the secretion of IL-1 $\beta$  into the cell supernatants of HEK293T cells co-transfected with the components of NLRP3 complex (Figure 5E). Overall, these data suggested that MPTR domain of PPE13 interacts with NLRP3 and enhances NLRP3 inflammasome activation.

## 4 | DISCUSSION

Previous studies suggested that pathogenic mycobacteria can activate the NLRP3 inflammasome, a process that is regulated by the secretion system ESX-1 and ESX-5. However, the mechanism and mycobacterial factors involved in NLRP3 inflammasome activation are poorly understood. In this study, we found that PPE13 facilitates NLRP3 inflammasome assembly and activation by interacting with NLRP3.

Previous studies indicated that *M. smegmatis* strain induces IL-1 $\beta$  secretion.<sup>34-36</sup> Our results showed that the recombinant *M. smegmatis* strain expressing PPE13 (named as Ms\_PPE13) enhanced cell death and IL-1 $\beta$  secretion in J774A.1, BMDMs, and THP-1 cells. PPE13 induces the transcription of pro-IL-1 $\beta$ , raising the possibility that increased IL-1 $\beta$  protein may be due to increased transcription. To exclude this possibility, we used CHX to inhibit new pro-IL-1 $\beta$  synthesis. Although the majority of the IL-1 $\beta$  released by BMDMs in response to Ms\_PPE13 was inhibited in the presence of CHX, Ms\_PPE13 still induced more IL-1 $\beta$  release compared to Ms\_Vec, suggesting that increased synthesis of pro-IL-1 $\beta$  in part accounts for the increased release of IL-1 $\beta$  by Ms\_PPE13. A previous study revealed that even *M. marinum* Esx-5 mutant reduced levels of pro-IL-1 $\beta$  synthesis compared to WT, failure of NLRP3 inflammasome activation by Esx-5 mutant mainly accounts for reduction of IL-1 $\beta$  release, as induction of high and equal expression of pro-IL-1 $\beta$  by adding LPS still resulted in strongly reduced IL-1 $\beta$  secretion in the ESX-5 mutant compared with that in the WT.<sup>18</sup> Given

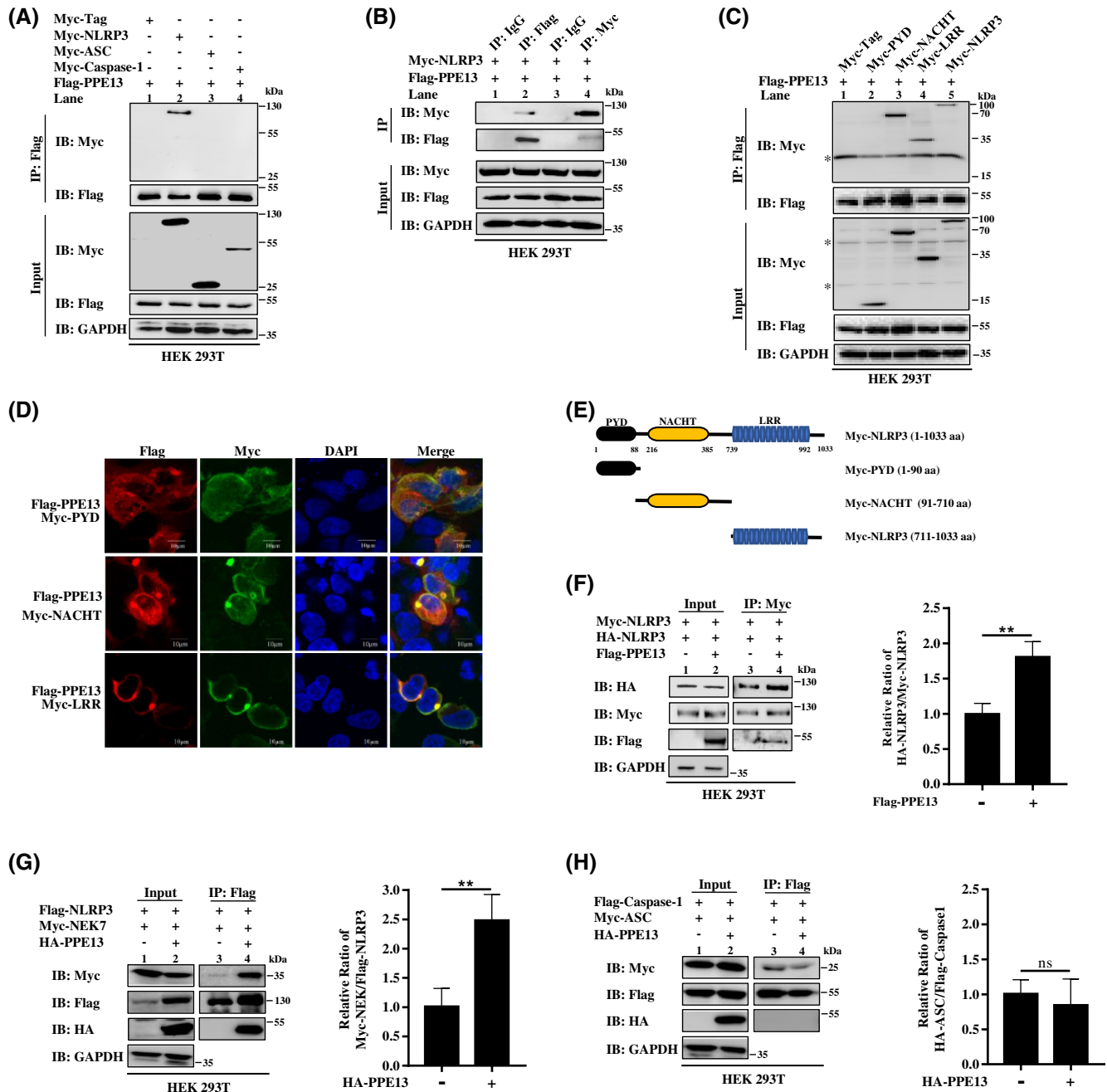


**FIGURE 4** PPE13 activates NLRP3 inflammasome by interacting with NLRP3. A, HEK293T cells were transfected with Flag-PPE13 together with Myc-Tag (an empty vector), Myc-NLRP3, Myc-ASC, or Myc-Caspase-1. Cell lysates were either directly analyzed by western blot using anti-Flag, anti-Myc, and anti-GAPDH antibodies (Input, lower panel), or were immunoprecipitated with anti-Flag antibody, and then, analyzed with anti-Flag and anti-Myc antibodies by western blot (IP, upper panel). B, HEK293T cells were transfected with Flag-PPE13 together with Myc-NLRP3. Cell lysates were immunoprecipitated with IgG, anti-Flag antibody, or anti-Myc antibody and then analyzed with anti-Flag and anti-Myc antibodies by western blot (IP, upper panel). C and D, HEK293T cells were transfected with Flag-PPE13 together with Myc-Tag (an empty vector), Myc-NLRP3 (full length), Myc-PYD, Myc-LRR, and Myc-NBD. C, Cell lysates were immunoprecipitated with anti-Flag antibody and then analyzed with anti-Flag and anti-Myc antibodies by western blot (IP, upper panel). Asterisk denotes nonspecific band. D, Subcellular localizations of Flag-PPE13 (red), Myc-proteins (green), and the nucleus marker DAPI (blue) were observed by confocal microscopy. Scale bar is 10 μm. E, Domain of structure and deletion constructs of NLRP3. F, G, and H, HEK293T cells were transfected with Myc-NLRP3, HA-NLRP3, and Flag-PPE13 (F); transfected with Flag-NLRP3, Myc-NEK7, and HA-PPE13 (G); transfected with Flag-Caspase-1, Myc-ASC, and HA-PPE13 (H). Cell lysates were immunoprecipitated with anti-Flag or anti-Myc antibody, and then, analyzed with anti-Flag, anti-HA, and anti-Myc antibodies by western blot (IP, upper panel). Densitometry was performed to analyze NLRP3 oligomerization, interaction between NLRP3 and NEK, interaction between ASC and caspase-1. Data are representative of three independent experiments. Values are mean ± SD, \*P < .05, \*\*P < .01, \*\*\*P < .001

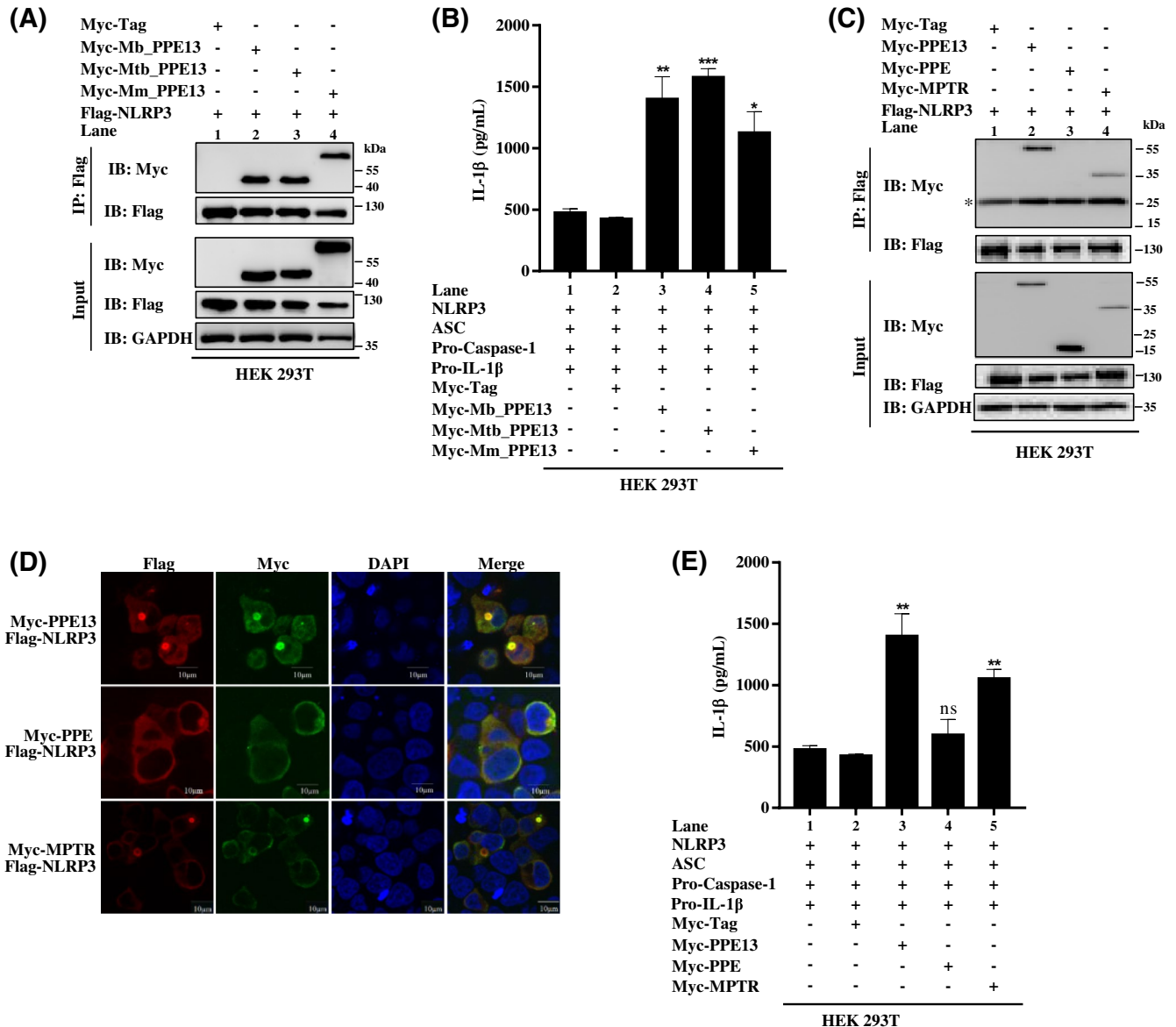


**FIGURE 5** PPE13 interacts with NLRP3 through its MPTR domain. A, HEK293T cells were transfected with Flag-NLRP3 together with Myc-Tag (an empty vector), Myc-Mb\_PPE13, Myc-Mtb\_PPE13, or Myc-Mm\_PPE13. Cell lysates were either directly analyzed by western blot using anti-Flag, anti-Myc, and anti-GAPDH antibodies (Input, bottom), or were immunoprecipitated with anti-Flag antibody and then analyzed with anti-Flag and anti-Myc antibodies by western blot (IP, top). B, HEK293T cells were transfected with plasmids encoding NLRP3, ASC, pro-Casp-1, pro-IL-1 $\beta$  together with Myc-Mb\_PPE13, Myc-Mtb\_PPE13, or Myc-Mm\_PPE13, respectively. C and D, HEK293T cells were transfected with Flag-NLRP3 along with Myc-Tag, Myc-PPE13 (full length), Myc-PPE domain, and Myc-MPTR domain. C, Cell lysates were immunoprecipitated with anti-Flag antibody and then analyzed with anti-Flag and anti-Myc antibodies by western blot (IP, top). Asterisk denotes nonspecific band. D, Subcellular localizations of Flag-NLRP3 (red), Myc-proteins (green), and the nucleus marker DAPI (blue) were observed by confocal microscopy. Scale bar is 10  $\mu$ m. E, HEK293T cells were transfected with plasmids encoding NLRP3, ASC, pro-Casp-1, and pro-IL-1 $\beta$  together with Myc-PPE or Myc-MPTR, respectively. Data are representative of three independent experiments. Values are mean  $\pm$  SD, \* $P$  < .05, \*\* $P$  < .01, \*\*\* $P$  < .001

that the increase of IL-1 $\beta$  secretion by Ms\_PPE13 was in a translation-independent manner, we further investigated the effect of Ms\_PPE13 on NLRP3 inflammasome activation. We found that treatment with caspase-1 specific inhibitor, z-YVAD-fmk, and NLRP3 inflammasome-specific inhibitor, MCC950, decreased Ms\_PPE13-induced IL-1 $\beta$  secretion in BMDMs, indicating that Ms\_PPE13-induced IL-1 $\beta$  secretion

is required for caspase-1 cleavage and NLRP3 inflammasome activation. This effect was further validated using NLRP3 deficient THP-1 cells, in which Ms\_PPE13-induced IL-1 $\beta$  secretion was inhibited.

Ms\_PPE13 induced more cleavage of GSDMD, which is regarded as an executor of pyroptosis.<sup>37</sup> IL-1 family cytokines have a diameter of 4.5 nm,<sup>38</sup> which is theoretically

narrow enough to pass through the GSDMD pore (inner diameter of 10–15 nm).<sup>39</sup> Interestingly, we observed that IL-1 $\beta$  release between Ms\_Vec and Ms\_PPE13 in THP-1 cells at 48 hours was not different. However, the expression of GSDMD p30 induced by Ms\_PPE13 increased eight times between 24 and 48 hours whereas the level of GSDMD p30 by Ms\_Vec increased almost eighty times, which may be the reason for observed changes in IL-1 $\beta$  release. Notably, we observed amount of IL-1 $\beta$  release into the supernatants of THP-1 at 6 hours during *M. smegmatis* infection, even though there was no cleavage of GSDMD detected at the same time. This indicated that we could not exclude the pyroptotic role of other members of the gasdermin family, like GSDMA, GSDMB, and GSDME, which also display pore-forming and pyroptotic activity.<sup>40–42</sup>

Further analysis revealed that PPE13 was localized to the surface of cells, which is consistent with results of a previous study.<sup>20</sup> The presence of PE/PPE proteins on the cell surface might enable them to directly interfere with host innate immune pathways.<sup>43</sup> Thus, we investigated whether PPE13 activates NLRP3 inflammasome directly or through other mycobacterial factors. We found that introduction of lentivirus expressing PPE13 significantly enhanced IL-1 $\beta$  secretion in THP-1 cells. The similar results also found in THP-1 cells stably expressing PPE13. Moreover, this enhanced IL-1 $\beta$  secretion was inhibited by z-YVAD-fmk and MCC950. We also showed PPE13 enhanced IL-1 $\beta$  secretion of in vitro NLRP3 inflammasome system reconstituted in HEK 293T cells. These findings indicate that PPE13 plays a direct role in NLRP3 inflammasome activation.

Recent studies suggest that PE/PPE proteins interact with TLR2 to modulate innate and adaptive immune response.<sup>44</sup> For example, PPE18 specifically interacts with TLR2, thereby stimulating IL-10 via the activation of p38 MAPK.<sup>45</sup> PPE60 directly binds to TLR2, induces DCs maturation and T-cell differentiation, as well as stimulates cytokines secretion. Other studies have shown that PPE60 can promote IL-1 $\beta$  secretion and activate NLRP3 inflammasome in a TLR2-dependent manner. However, knock-out of TLR2 did not completely abrogate the expression of NLRP3 protein and the secretion of IL-1 $\beta$  induced by PPE60, indicating that other receptors may contribute to NLRP3 inflammasome activation.<sup>46</sup> Interestingly, we found that PPE13 can directly interact with NLRP3 protein, but not with ASC and caspase-1.

Upon activation, NLRP3 undergoes conformational changes leading to oligomerization, which enables it to assemble with ASC, and subsequent recruitment of procaspase-1 via CARD-CARD interaction. Clustered procaspase-1 is autocleaved to active caspase-1 (p10/20), which triggers the maturation of IL-1 $\beta$ .<sup>47</sup> NLRP3 protein contains three domains, namely, PYD, NACHT, and LRR domain. PYD domain is required for NLRP3 and ASC interaction. ATPase activity in NACHT domain is important for NLRP3

oligomerization and activation.<sup>48</sup> NEK7 is newly identified NLRP3 inflammasome component which binds to LRR domain of NLRP3 to facilitate its assembly.<sup>49</sup> Our results showed that PPE13 interacts with the NACHT and LRR domains of NLRP3. We also showed that PPE13 promotes NLRP3-ASC, NLRP3-NLRP3, and NEK7-NLRP3 interaction, as well as the oligomerization of ASC in the presence of NLRP3. Taken together, this study demonstrates that PPE13 activates NLRP3 inflammasome by facilitating NLRP3 inflammasome assembly, a process that might be achieved by NLRP3.

Recent studies demonstrated that the posttranslational modifications (PTMs), including phosphorylation, ubiquitination, and deubiquitylation, regulate NLRP3 inflammasome activation. For example, BRCC3 targets the LRR domain of NLRP3 to promote NLRP3 inflammasome activation by deubiquitylation.<sup>50</sup> PTPN22 interacts with NLRP3 and dephosphorylates it at Tyr861 in the LRR domain, leading to efficient NLRP3 inflammasome activation and IL-1 $\beta$  secretion.<sup>51</sup> Yet, whether PTMs of NLRP3 are part of the molecular mechanisms by which PPE13 facilitates NLRP3 inflammasome assembly remains to be determined.

Pathogenic mycobacteria triggers inflammasome activation, and thus, IL-1 $\beta$  secretion in T7SS-dependent manner.<sup>10,12,13</sup> The role of ESX-1 in inflammasome activation has been extensively studied. ESX-1 mutant strains of pathogenic mycobacteria failed to activate AIM2 and NLRP3 inflammasomes, due to the inability of bacteria to translocate from phagosome to cytosol.<sup>10,12,13</sup> Interestingly, ESX-5 mutants fail to activate the NLRP3 inflammasome and promote IL-1 $\beta$  secretion, even though ESX-5 mutants are able to escape from the phagolysosome into the cytosol.<sup>17–19</sup> This observation indicated that ESX-1 is needed for the cytosolic localization, which allows ESX-5 effector molecules to be secreted in the cytosol to manipulate immune response. It is therefore conceivable that PPE13 protein can interact with NLRP3 of host cells during infection after phagolysosome escape. Interaction of surface-exposure members of PE/PPE family with molecules in the host cytosol during infection has been previously described. For instance, PE\_PGERS33 interacts with the mitochondria to affect cell death during infection,<sup>52</sup> whereas PE\_PGERS protein Rv0297 localizes to endoplasmic reticulum to mediate apoptosis.<sup>53</sup> Clearly, future experiments are required to unravel the mechanism on interaction between PPE13 and NLRP3 during natural infection. In the present study, we found that all the PPE13 proteins from *M. bovis*, *M. tuberculosis*, and *M. marinum* activate NLRP3 inflammasome through binding to NLRP3. PPE13 belongs to PPE\_MPTR (major polymorphic tandem repeat) subfamily, which is characterized by multiple C-terminal repeats of motif NxGxNxG.<sup>26,54</sup> The highly repetitive domain of PPE\_MPTR families is primarily responsible for induction

of antibody responses.<sup>55</sup> More interestingly, we demonstrated that PPE13 activates NLRP3 inflammasome and interacts with NLRP3 through repetitive MPTR domain but not through conserved PPE domain.

In summary, our study demonstrates that PPE13 triggers NLRP3 inflammasome activation and IL-1 $\beta$  secretion. More importantly, PPE13 interacts directly with NLRP3 to facilitate assembly of NLRP3 inflammasome, and this interaction requires NACHT and LRR domains of NLRP3 as well as the MPTR domain of PPE13. These datasets reveal a new role of PPE13 in the activation of NLRP3 inflammasome. PPE13 may be a new candidate which can be used to unravel the mechanism of ESX-5-mediated IL-1 $\beta$  secretion.

## ACKNOWLEDGMENTS

We thank Prof. Michael Niederweis from University of Alabama at Birmingham for providing the vector pMS2 used in this study. The work was funded by the National Natural Science Foundation of China (Grant Nos. 31502034, 31502127, 31602119, 31602062, 31770040, 31802258, 31902249, and 31972648), Natural Science Foundation of Zhejiang Province (Grant Nos. LQ15C180002, LQ19C180003, LQ20C180002, and LZ19C180001), the key Research and Development Program of Zhejiang Province (Grant No. 2019C02043) and ZAFU talents starting program (Grant Nos. 2014FR069).

## CONFLICT OF INTEREST

The authors declare that they have no financial or commercial conflict of interest.

## AUTHOR CONTRIBUTIONS

Y. Yang, Y. Zhou, Q. Song, and B. Zhou designed research; P. Xu, P. He, and Y. Tang performed research; C. Guan, H. Zeng, S. Jiang, C. Shao, J. Sun, Y. Yang, X. Wang, and H. Song analyzed data; Y. Yang, F. Shi, and H. Song wrote the paper.

## REFERENCES

- World Health Organization. *Global tuberculosis report 2018*. Geneva, Switzerland: WHO; 2018.
- Cooper AM, Mayer-Barber KD, Sher A. Role of innate cytokines in mycobacterial infection. *Mucosal Immunol*. 2011;4:252-260.
- Juffermans N, Florquin S, Camoglio L, et al. Interleukin-1 signaling is essential for host defense during murine pulmonary tuberculosis. *J Infect Dis*. 2000;182(3):902-908.
- Yamada H, Mizuno S, Horai R, Iwakura Y, Sugawara I. Protective role of interleukin-1 in mycobacterial infection in IL-1 a/b double-knockout mice. *Lab Invest*. 2000;80(5):759-767.
- Sugawara I, Yamada H, Hua S, Mizuno S. Role of interleukin (IL)-1 type 1 receptor in mycobacterial infection. *Microbiol Immunol Microbiol Immunol*. 2001;45(11):743-750.
- Fremont CM, Togbe D, Doz E, et al. IL-1 receptor-mediated signal is an essential component of MyD88-dependent innate response to *Mycobacterium tuberculosis* infection. *J Immunol*. 2007;179:1178-1189.
- Mayer-Barber KD, Andrade BB, Barber DL, et al. Innate and adaptive interferons suppress IL-1 $\alpha$  and IL-1 $\beta$  production by distinct pulmonary myeloid subsets during *Mycobacterium tuberculosis* infection. *Immunity*. 2011;35:1023-1034.
- Mayer-Barber KD, Andrade BB, Oland SD, et al. Host-directed therapy of tuberculosis based on interleukin-1 and type I interferon crosstalk. *Nature*. 2014;511:99-103.
- Latz E, Xiao TS, Stutz A. Activation and regulation of the inflammasomes. *Nat Rev Immunol*. 2013;13:397-411.
- Saiga H, Kitada S, Shimada Y, et al. Critical role of AIM2 in *Mycobacterium tuberculosis* infection. *Int Immunol*. 2012;24:637-644.
- Yang Y, Zhou X, Kouadir M, et al. the AIM2 inflammasome is involved in macrophage activation during infection with virulent *Mycobacterium bovis* strain. *J Infect Dis*. 2013;208:1849-1858.
- Koo IC, Wang C, Raghavan S, et al. ESX-1-dependent cytolysis in lysosome secretion and inflammasome activation during mycobacterial infection. *Cell Microbiol*. 2008;10:1866-1878.
- Carlsson F, Kim J, Dumitru C, et al. Host-detrimental role of Esx-1-mediated inflammasome activation in mycobacterial infection. *PLoS Pathog*. 2010;6:e1000895.
- Kurenuma T, Kawamura I, Hara H, et al. The RD1 locus in the *Mycobacterium tuberculosis* genome contributes to activation of caspase-1 via induction of potassium ion efflux in infected macrophages. *Infect Immun*. 2009;77:3992-4001.
- Mishra BB, Moura-Alves P, Sonawane A, et al. *Mycobacterium tuberculosis* protein ESAT-6 is a potent activator of the NLRP3/ASC inflammasome. *Cell Microbiol*. 2010;12:1046-1063.
- Wassermann R, Gulen M, Sala C, et al. *Mycobacterium tuberculosis* differentially activates cGAS- and inflammasome-dependent intracellular immune responses through ESX-1. *Cell Host Microbe*. 2015;17:799-810.
- Abdallah AM, Savage ND, van Zon M, et al. The ESX-5 secretion system of *Mycobacterium marinum* modulates the macrophage response. *J Immunology*. 2008;181:7166-7175.
- Abdallah AM, Bestebroer J, Savage ND, et al. Mycobacterial secretion systems ESX-1 and ESX-5 play distinct roles in host cell death and inflammasome activation. *J Immunol*. 2011;187:4744-4753.
- Shah S, Cannon JR, Fenselau C, Briken V. A Duplicated ESAT-6 region of ESX-5 is involved in protein export and virulence of mycobacteria. *Infect Immun*. 2015;83:4349-4361.
- Abdallah AM, Verboom T, Weerdenburg EM, et al. PPE and PE\_PGRS proteins of *Mycobacterium marinum* are transported via the type VII secretion system ESX-5. *Mol Microbiol*. 2009;73:329-340.
- Ahmed A, Das A, Mukhopadhyay S. Immunoregulatory functions and expression patterns of PE/PPE family members: roles in pathogenicity and impact on anti-tuberculosis vaccine and drug design. *IUBMB Life*. 2015;67:414-427.
- Sampson SL, Lukey P, Warren RM, et al. Expression, characterization and subcellular localization of the *Mycobacterium tuberculosis* PPE gene Rv1917c. *Tuberculosis*. 2001;81:305-317.
- Malen H, Pathak S, Softeland T, de Souza GA, Wiker HG. Definition of novel cell envelope associated proteins in Triton X-114 extracts of *Mycobacterium tuberculosis* H37Rv. *BMC Microbiol*. 2010;10:132.

24. Demangel C, Brodin P, Cockle PJ, et al. Cell envelope protein PPE68 contributes to *Mycobacterium tuberculosis* RD1 immunogenicity independently of a 10-kilodalton culture filtrate protein and ESAT-6. *Infect Immun*. 2004;72:2170-2176.
25. Adindla S, Guruprasad L. Sequence analysis corresponding to the PPE and PE proteins in *Mycobacterium tuberculosis* and other genomes. *J Biosci*. 2003;28:169-179.
26. Hermans PW, van Soolingen D, van Embden JD. Characterization of a major polymorphic tandem repeat in *Mycobacterium tuberculosis* and its potential use in the epidemiology of *Mycobacterium kansasii* and *Mycobacterium goodii*. *J Bacteriol*. 1992;174:4157-4165.
27. Cubillos-Ruiz A, Morales J, Zambrano MM. Analysis of the genetic variation in *Mycobacterium tuberculosis* strains by multiple genome alignments. *BMC Res Notes*. 2008;1:110.
28. Soldini S, Palucci I, Zumbo A, et al. PPE\_MPTR genes are differentially expressed by *Mycobacterium tuberculosis* in vivo. *Tuberculosis*. 2011;91:563-568.
29. Stewart GR, Patel J, Robertson BD, Rae A, Young DB. Mycobacterial mutants with defective control of phagosomal acidification. *PLoS Pathog*. 2005;1:269-278.
30. Thi EP, Hong CJ, Sanghera G, Reiner NE. Identification of the *Mycobacterium tuberculosis* protein PE-PGRS62 as a novel effector that functions to block phagosome maturation and inhibit iNOS expression. *Cellular Microbiol*. 2013;15:795-808.
31. Gey van Pittius NC, Sampson SL, Lee H, et al. Evolution and expansion of the *Mycobacterium tuberculosis* PE and PPE multigene families and their association with the duplication of the ESAT-6 (*esx*) gene cluster regions. *BMC Evol Biol*. 2006;6:95.
32. Mariathasan S, Monack DM. Inflammasome adaptors and sensors: intracellular regulators of infection and inflammation. *Nat Rev Immunol*. 2007;7:31-40.
33. Coll RC, Robertson AAB, Chae JJ, et al. A small-molecule inhibitor of the NLRP3 inflammasome for the treatment of inflammatory diseases. *Nat Med*. 2015;21:248-255.
34. Shah S, Bohsali A, Ahlbrand SE, et al. Cutting edge: *Mycobacterium tuberculosis* but not nonvirulent mycobacteria inhibits IFN- $\beta$  and AIM2 inflammasome-dependent IL-1 $\beta$  production via its ESX-1 secretion system. *J Immunol*. 2013;191:3514-3518.
35. Feng Z, Bai X, Wang T, et al. Differential responses by human macrophages to infection with *Mycobacterium tuberculosis* and non-tuberculous mycobacteria. *Front Microbiol*. 2020;11:116.
36. Mi Y, Bao L, Gu D, et al. *Mycobacterium tuberculosis* PPE25 and PPE26 proteins expressed in *Mycobacterium smegmatis* modulate cytokine secretion in mouse macrophages and enhance mycobacterial survival. *Res Microbiol*. 2017;168:234-243.
37. Galluzzi L, Vitale I, Aaronson SA, et al. Molecular mechanisms of cell death: recommendations of the nomenclature committee on cell death 2018. *Cell Death Differ*. 2018;25:486-541.
38. van Oostrum J, Priestle JP, Grutter MG, Schmitz A. The structure of murine interleukin-1  $\beta$  at 2.8 Å resolution. *J Struct Biol*. 1991;107:189-195.
39. Liu X, Zhang Z, Ruan J, et al. Inflammasome-activated gasdermin D causes pyroptosis by forming membrane pores. *Nature*. 2016;535:153-158.
40. Ding J, Wang K, Liu W, et al. Pore-forming activity and structural autoinhibition of the gasdermin family. *Nature*. 2016;535:111-116.
41. Zhou Z, He H, Wang K, et al. Granzyme A from cytotoxic lymphocytes cleaves GSDMB to trigger pyroptosis in target cells. *Science*. 2020;368:eaaz7548.
42. Wang Y, Gao W, Shi X, et al. Chemotherapy drugs induce pyroptosis through caspase-3 cleavage of a gasdermin. *Nature*. 2017;547:99-103.
43. Sayes F, Pawlik A, Frigui W, et al. CD4+ T cells recognizing PE/PPE antigens directly or via cross reactivity are protective against pulmonary mycobacterium tuberculosis infection. *PLoS Pathog*. 2016;12:e1005770.
44. Sampson SL. Mycobacterial PE/PPE proteins at the host-pathogen interface. *Clin Dev Immunol*. 2011;2011:497203.
45. Nair S, Ramaswamy PA, Ghosh S, et al. The PPE18 of *Mycobacterium tuberculosis* interacts with TLR2 and activates IL-10 induction in macrophage. *J Immunol*. 2009;183:6269-6281.
46. Su H, Zhang Z, Liu Z, et al. *Mycobacterium tuberculosis* PPE60 antigen drives Th1/Th17 responses via Toll-like receptor 2-dependent maturation of dendritic cells. *J Biol Chem*. 2018;293:10287-10302.
47. Schroder K, Tschopp J. The inflammasomes. *Cell*. 2010;140:821-832.
48. Duncan JA, Bergstralh DT, Wang Y, et al. Cryopyrin/NALP3 binds ATP/dATP, is an ATPase, and requires ATP binding to mediate inflammatory signaling. *Proc Natl Acad Sci USA*. 2007;104:8041-8046.
49. Shi H, Wang Y, Li X, et al. NLRP3 activation and mitosis are mutually exclusive events coordinated by NEK7, a new inflammasome component. *Nat Immunol*. 2016;17:250-258.
50. Py BF, Kim MS, Vakifahmetoglu-Norberg H, Yuan J. Deubiquitination of NLRP3 by BRCC3 critically regulates inflammasome activity. *Mol Cell*. 2013;49:331-338.
51. Spalinger MR, Kasper S, Gottier C, et al. NLRP3 tyrosine phosphorylation is controlled by protein tyrosine phosphatase PTPN22. *J Clin Invest*. 2016;126:1783-1800.
52. Cadieux N, Parra M, Cohen H, et al. Induction of cell death after localization to the host cell mitochondria by the *Mycobacterium tuberculosis* PE\_PGRS33 protein. *Microbiology*. 2011;157:793-804.
53. Grover S, Sharma T, Singh Y, et al. The PGRS domain of *Mycobacterium tuberculosis* PE\_PGRS protein Rv0297 is involved in endoplasmic reticulum stress-mediated apoptosis through toll-like receptor 4. *MBio*. 2018;9:e01017-18.
54. Adindia S, Guruprasad L. Sequence analysis corresponding to the PPE and PE proteins in *Mycobacterium tuberculosis* and other genomes. *J Biosci*. 2003;28:169-179.
55. Chakhaiyar P, Nagalakshmi Y, Aruna B, et al. Regions of high antigenicity within the hypothetical PPE major polymorphic tandem repeat open-reading frame, Rv2608, show a differential humoral response and a low T cell response in various categories of patients with tuberculosis. *J Infect Dis*. 2004;190(7):1237-1244.

## SUPPORTING INFORMATION

Additional Supporting Information may be found online in the Supporting Information section.

**How to cite this article:** Yang Y, Xu P, He P, et al. Mycobacterial PPE13 activates inflammasome by interacting with the NATCH and LRR domains of NLRP3. *The FASEB Journal*. 2020;34:12820–12833. <https://doi.org/10.1096/fj.202000200RR>